

Original Article

A topical Chinese herbal inhibits pruritus and skin inflammation via neural TRPM8 in atopic dermatitis

Yao Chen^{a,†}, Ziyuan Tang^{a,†}, Zhiyao Han^a, Mingyang Wang^a, Xinran Li^a,
Luying Lai^a, Pingzheng Zhou^{a,b}, Fang Wang^{c,d,*}, Fengxian Li^{a,e,**,‡}

^a Department of Anesthesiology, Zhujiang Hospital, Southern Medical University, Guangzhou, China

^b Guangdong Provincial Key Laboratory of New Drug Screening, School of Pharmaceutical Sciences, Southern Medical University, Guangzhou, China

^c Department of Dermatology, Dermatology Hospital, Southern Medical University, Guangzhou, China

^d Guangdong Provincial Key Laboratory of Brain Function and Disease, Guangzhou, China

^e Key Laboratory of Mental Health of the Ministry of Education, Guangdong Province Key Laboratory of Psychiatric Disorders, Southern Medical University, Guangzhou, China



ARTICLE INFO

Keywords:

Atopic dermatitis
TRPM8
Pruritus
Inflammation
Chinese herb

ABSTRACT

Background: Atopic dermatitis (AD) is a chronic, itchy, and inflammatory skin disease. The neuroimmune concept of itch involves aberrant immune responses and neural activities. Chinese herbal medicine has been demonstrated to alleviate AD symptoms, but the underlying mechanisms remain not fully understood.

Purpose: Chushizhiyang (CS) ointment is a topical treatment consisting of Chinese herbal ingredients. We aimed to study the underlying mechanism of CS on treating AD.

Method: To investigate the therapeutic efficacy of CS, we utilized a well-established atopic dermatitis mouse model, administering CS ointment topically to the ears. To unravel the underlying mechanisms, we employed a multifaceted approach, including behavioral assay, network pharmacology analysis, RNA-sequencing analysis, neural tracing, and calcium imaging. Additionally, transient receptor potential (TRP) M8-deficient mice were employed to validate the specific targets of CS.

Results: By employing a murine model of AD-like disease, we found that CS ointment can reduce skin inflammation and inhibit scratching behavior. Importantly, its capacity to alleviate itch-induced scratching surpasses that of topical steroid, a positive control treatment. The RNA-sequencing analysis of the affected skin revealed that the differentially expressed genes were enriched in neuroactive pathways that include ion channels particularly TRPM8. Calcium imaging demonstrated that CS ointment is capable of activating TRPM8-positive sensory neurons. Using transgenic animals, we found that CS ointment exhibited its anti-inflammatory or anti-pruritic effects only when TRPM8 is functional intact. Additionally, CS treatment reduced neuronal activities in wild-type, rather than TRPM8-compromised animals.

Conclusion: Our findings suggest that topical Chinese herbals participate in neuroimmune mechanisms for AD-like disease via TRPM8.

Abbreviations: AD, atopic dermatitis; TRPM8, transient receptor potential M8; CS, Chushizhiyang ointment; EtOH, ethanol; HPLC, high performance liquid chromatography; TCMS, traditional Chinese medicine systems pharmacology database; PPI, protein-protein interaction; GO, Gene Ontology; KEGG, Kyoto Encyclopedia of Genes and Genomes; IL-4, interleukin-4; IL-13, interleukin-13; IL-31, interleukin-31; IL-33, interleukin-33; CCL17, C-C Motif Chemokine Ligand 17; TSLP, thymic stromal lymphopoietin; eGFP, enhanced green fluorescence protein; FG, fluoro-gold; DRG, dorsal root ganglion; TG, trigeminal ganglion; pERK, phosphorylated extracellular signal-regulated kinase.

** Corresponding author: Zhujiang Hospital, Southern Medical University, No. 253 Gongye Rd, Guangzhou 510282, China.

* Corresponding author: Dermatology Hospital, Southern Medical University, No. 2 Lujing Road, Guangzhou, Guangdong 510095, China.

E-mail addresses: wangf78@mail.sysu.edu.cn (F. Wang), lifengxian81@smu.edu.cn (F. Li).

† Yao Chen and Ziyuan Tang contributed equally to this work.

‡ Lead Contact.

<https://doi.org/10.1016/j.phymed.2025.156524>

Received 7 September 2024; Received in revised form 12 February 2025; Accepted 15 February 2025

Available online 16 February 2025

0944-7113/© 2025 The Authors. Published by Elsevier GmbH. This is an open access article under the CC BY license (<http://creativecommons.org/licenses/by/4.0/>).

Introduction

Atopic dermatitis (AD) is recognized as the most common chronic inflammatory skin disease, characterized by relapsing eczematous lesions, intense itch, and epidermal barrier dysfunction (Ständer, 2021). The Global Burden of Disease study estimates the worldwide prevalence of AD to be between 15 % and 20 % (Laughter et al., 2021). AD imposes a substantial disease burden on patients, ranking as the leading nonfatal dermatological condition that impairs quality of life (Peng et al., 2022). Recent research has enhanced our understanding of AD's complex mechanisms, emphasizing the roles of skin environments, barrier function, and neuroimmune interactions (Luger et al., 2021).

Current treatment approaches for AD encompass topical and systemic medications (Wollenberg et al., 2022). Topical therapies include corticosteroids, calcineurin inhibitors (e.g., tacrolimus and pimecrolimus), and phosphodiesterase 4 inhibitors, which are available on the market (Eichenfield et al., 2014; Li et al., 2021). However, these therapies can be limited by varying effectiveness and adverse effects such as irritation and burning, which may deter patient adherence. Traditional Chinese herbal medicine, derived from medicinal herbs and plants, provides an alternative strategy for treating AD (Wang et al., 2023), but the underlying mechanisms are not well identified due to the complexity of the ingredients.

The skin is densely innervated by primary sensory nerves, which are the first to sense various somatosensation, including touch, temperature, pain, and itch. Itch signals are initiated at nerve endings through the binding of specific receptors, leading to membrane depolarization via the opening of cation channels, such as transient receptor potential (TRP) channels. TRPM8, known as the cold and menthol receptor, is a TRP family ion channel that is extensively expressed in sensory neurons. Activation of TRPM8 has been shown to reduce itch scratching in murine models (Liu and Jordt, 2018), and clinical studies have revealed that a TRPM8 agonist, menthoxyethylene glycol, can significantly alleviate itch in AD patients (Misery et al., 2019). Thus, TRPM8 may serve as a promising therapeutic target for managing itch symptoms in AD.

Emerging studies have highlighted neuroimmune interactions in various conditions (Chu et al., 2020; Huang et al., 2023). Inflammatory mediators released by immune cells can activate neurons, while activated neurons produce neuropeptides and neurotransmitters that act on immune cells. The concept of "itch that rashes" in AD suggests a neuroimmune paradigm, where itch-provoked scratching can aggregate skin barrier dysfunction and inflammation (Mack and Kim, 2018). Research by Wang et al. (2020) has demonstrated that the activation of TRPM8 with thymol can reduce skin inflammation in a mouse model of psoriasis (Wang et al., 2020), suggesting a role for neuronal TRPM8 in controlling skin inflammation.

Chushizhiyang (CS) ointment, developed from traditional Chinese herbal components, has been approved for AD treatment in China. Chinese herbal medicine has shown efficacy in improving skin lesions and itch in patients with eczema (Cai et al., 2022; Wang et al., 2023). Using an AD murine model, we demonstrate that CS ointment effectively mitigates skin inflammation, blood vessel dilation, and itch scratching. Importantly, we reveal that CS ointment has the capacity to activate TRPM8, which mediates its anti-inflammation and anti-itch effects in AD.

Materials and methods

Animals

All animal experimental protocols were reviewed and approved by the Ethics Committee of Zhujiang Hospital, Southern Medical University (Protocol: LAEC-2022-202, approval date: 12/27/2022). Wild-type (WT) C57BL/6J mice were purchased from GemPharmatech Co., Ltd (Nanjing, China). *Trpm8*^{EGFPj} mice were generously provided by Dr. Zongxiang Tang from the Department of Physiology, School of

Medicine, Nanjing University of Chinese Medicine. Mice were housed under a 12/12-hour light/dark cycle and maintained in specific-pathogen-free environment. Observers were blinded to genotypes during testing procedures.

MC903-induced AD-like mouse model

An AD-like dermatitis model in mice was induced by a topical application of 2 nmol of MC903 (calcipotriol, 2700/10, R&D Systems) in 10 μ L 100 % ethanol to the bilateral ear skin. MC903 treatment was administered daily from day 1 to day 7, with a single dose on day 11 to induce flare-ups. Ethanol alone was applied as control at corresponding time-points. Mouse ear thickness was measured daily from day 0 to day 14 using vernier calipers (G1-A, Peacock, Japan).

Treatment for AD-like model

AD-like mice were treated with topical drugs twice daily from day 8 to day 14 using vehicle, CS and hydrocortisone according to subgroups. Vehicle ointment (Yifan Pharmaceutical, China) as a negative control does not contain herbal ingredients consisting of sodium dodecyl sulfate, glycerin, hydroxyphenethyl ester, petroleum jelly, and hexadecanol. Chushizhiyang ointment (Z20103068, Yifan Pharmaceutical, China) contains herbal ingredients that are *Cnidii Fructus*, *Coptidis Rhizoma*, *Phellodendri Chinensis Cortex*, *Dictamni Cortex*, *Sophorae Flavescentis Radix*, *Polygoni Cuspidati Rhizoma et Radix*, *Viola Herba*, *Kochiae Fructus*, *Polygoni Avicularis Herba*, *Artemisiae Scopariae Herba*, *Atractylodis Rhizoma*, *Zanthoxylum bungeanum*, and *Borneol*. 0.5X CS ointment was prepared by mixing vehicle ointment and CS ointment in a 1:1 ratio by weight. Hydrocortisone butyrate cream (Tianjin Jin Yao Pharmaceutical Co., China) at a concentration of 0.1 % was used as a positive control.

Scratching behavior assessment

Behavioral tests were conducted by experimenters blinded to genotypes. Video recordings were manually scored to determine the number of scratching bouts. A scratching bout was defined as an episode of continuous scratching of the ears with the hind paw, ceasing when the mouse placed their hind paw in its mouth or on the chamber floor.

Network pharmacology

Protein targets of CS ointment were retrieved from the Traditional Chinese Medicine Systems Pharmacology Database (TCMSP) using the components of CS ointment, with a drug-likeness threshold set at greater than 0.18. Protein targets associated with AD were obtained from Gene Cards (<https://www.genecards.org>), OMIM (<https://www.omim.org/>) and DisGeNET (<https://disgenet.com/>) using "atopic dermatitis" as keyword. Protein-protein interactions (PPIs) of the shared protein targets in CS ointment and AD were analyzed using STRING (<https://string-db.org>) and visualized in Cytoscape (ver.3.10.2). Gene Ontology (GO) and Kyoto Encyclopedia of Genes and Genomes (KEGG) pathway enrichment analyses were performed using OmicStudio tools (<https://www.omicstudio.cn>). Biological processes (BP), cellular components (CC), molecular functions (MF) and key signaling pathway were identified to elucidate the potential mechanisms of CS ointment in treating AD.

Measurement of ear skin microvascular perfusion

Mice were anesthetized with 2 % isoflurane, and the ear was flattened with coverslip. Blood flow was recorded for 1 min using the laser speckle contrast imaging system (SIM BFI-HR Pro, Hubei, China). Blood perfusion signal was displayed as a color-coded image and analyzed as numerical perfusion unit (PU).

HPLC fingerprint for CS quality control

CS samples (2.0 g) were ultrasonically extracted in 75 % ethanol (50 mL, 40 kHz, 300 W, 30 min), filtered, and analyzed using an Agilent 1260 HPLC system with a Xtimate C18 column (4.6 × 250 mm, 5 μm). The mobile phase comprised acetonitrile (A) and 0.1 % phosphoric acid (B) with the following gradient: 5–30 % A (0–35 min), 30–40 % A (35–45 min), 40–90 % A (45–90 min) at 1.0 mL/min. Detection was at 280 nm (35 °C, 10 μL injection). Six bioactive components were identified: chlorogenic acid, esculetin, polydatin, berberine, emodin, and osthole, establishing a reliable quality control for CS.

Hematoxylin-eosin staining

Ear skin tissues were collected post-euthanized via CO₂ and fixed with 4 % paraformaldehyde (PFA) in PBS overnight before paraffin embedding. Tissue sections (4–5 mm) were stained with hematoxylin and eosin and imaged by a slide scanner (Pannoramic MIDI II, 3D HISTECH, Hungary). Ear epidermal thickness was quantified using SlideViewer software.

Immunofluorescence staining

For immunohistochemical staining, mice were euthanized with CO₂ and perfused with ice-cold PBS (pH 7.4) followed by 4 % PFA in PBS. Tissues were collected, post-fixed with 4 % PFA for 30 mins, and cryoprotected in 30 % (w/v) sucrose overnight at 4 °C. OCT-embedded tissues were then sectioned at 15 μm and blocked with 10 % goat serum in PBS with 0.1 % triton for one hour before primary antibody incubation overnight at 4 °C. Secondary antibody incubation was performed for one hour after washing out the primary antibodies. Images were acquired using a confocal scanning laser microscope (Ax, Nikon, Tokyo) and analyzed by NIS software. Primary antibodies: rabbit anti-pERK (4370T, CST, 1:1000), chicken anti-GFP (GFP-1020, Aves Labs, 1:1000). Second antibodies: goat anti-rabbit 555 (A21429, ThermoFisher, 1:1000), donkey anti-chicken 488 (703–546–155, Jackson Immuno Research, 1:1000).

ELISA

Mouse ear tissue (40 mg) was homogenized in a grinding tube containing 3 μL of ProtLytic protease and phosphatase inhibitor cocktail (New Cell & Molecular Biotech Co.,Ltd), and 297 μL of RIPA (WB3100, New Cell & Molecular Biotech Co.,Ltd) at 60–70 Hz at -20 °C. The homogenate was centrifuged at 12,000 rpm at 4 °C for 10 mins, and the supernatant was collected. IL-4, IL-13 and IL-31 were tested using mouse ELISA kit (IL-4, ELM-IL4–1; IL-13, ELM-IL13–1; IL-31, ELM-IL31–1, RayBiotech) according to the manufacturer's instructions.

mRNA-sequencing analysis

Total RNA was isolated and purified from mouse ear using TRIzol reagent (Invitrogen, Carlsbad, CA, USA). mRNA-sequencing and library preparation were performed by LC-Bio Technology CO., Ltd. Raw RNA-sequencing data were processed using HISAT2 (<https://ccb.jhu.edu/software/hisat2>) and StringTie (<https://ccb.jhu.edu/software/stringtie>). Differentially expressed mRNAs were selected with fold change > 1.5 or fold change < 0.67 and with parametric F-test comparing nested linear models (FDR < 0.05) by R package edgeR (<https://bioconductor.org/packages/release/bioc/html/edgeR.html>). Volcano plots were generated using the LC-Bio Technology website (<https://www.omicstudio.cn/home>). KEGG gene enrichment analysis was performed using DAVID software (<https://david.ncicrf.gov/>).

Real-time RT-PCR analysis

On day 14 at the end of treatment, mouse ear tissue was collected for RT-PCR. Total RNA was isolated and analyzed using TRIzol reagent. Then, the RNA was reverse transcribed into cDNA by using a Reagent (Q202–00, EnzyArtisan, China) following the manufacturer's procedures. RT-PCR was performed on Real-time PCR Detection System (LC480, Roche, USA) using reagent (Q204–01, EnzyArtisan, China). The mRNA levels were normalized to the level of β-actin. The primer sequences used for PCR were as follows: β-actin: F-GTGCTATGTTGCTC-TAGACTTCG and R-ATGCCACAGGATTCCATACC; IL-4: F-TACCAGGA GCCATATCCACGGATG and R-TGTGGTGTCTTCGTTGCTGTGAG; IL-13: F-ACCCTTAAGGAGCTTATTGAGG and R-ATTGCAATTGGAGATGTTGGTC; IL-31: F-TCAGCAGACGAATCAATACAGC and R-TCGTCAACACTTTGACTTTCT; IL33: F-CAGAAGACCAAAGAATTC TGCC and R-CATGCTTGGTACCCGATTTAG; Tslp: F- ACTGCAACTT-CACGTCAATTAC and R- CGAACTTAGCCCTTTCAAATC; Ccl17: F-AGGTCACCTCAGATGCTGCTC and R- ACTCTCGGCCTACATTGGTG; Trpm8: F- CAAAACACCCAACCTGGTCATTTC and R- CACAGTGC GTGGTAAAAAGCG.

Retrograde study

Mice were anesthetized with 250 mg/kg tribromoethanol, and fluoro-gold (80,014, Biotium, 2 % diluted in ddH₂O) was injected intradermally (10 μL) into the ear skin. Five days later, DRGs from C1-C3 and TG were collected for immunofluorescence staining after mice euthanized with CO₂.

Calcium imaging of mouse sensory neurons

Primary sensory neurons were dissociated and cultured overnight at 37 °C, 5 % CO₂, as described previously (Li et al., 2019). Neurons were maintained in DMEM-F12 (Corning, NY, USA) containing 10 % fetal bovine serum (Gibco, CA, USA), 1 % penicillin and 1 % streptomycin util testing. For calcium imaging, neurons were incubated with fura-2AM (F1221, Fisher Scientific) in calcium imaging buffer (2 μg/mL) for 40 mins at room temperature. After a 10-minutes recovery period, neurons were imaged at 340 and 380 nm excitation to detect calcium response. Calcium response was captured using an inverted Nikon fluorescence microscope equipped with a cooled sCMOS camera (pco.edge 4.2, Germany). A 15 % increase in the 340/380 ratio was considered as a response.

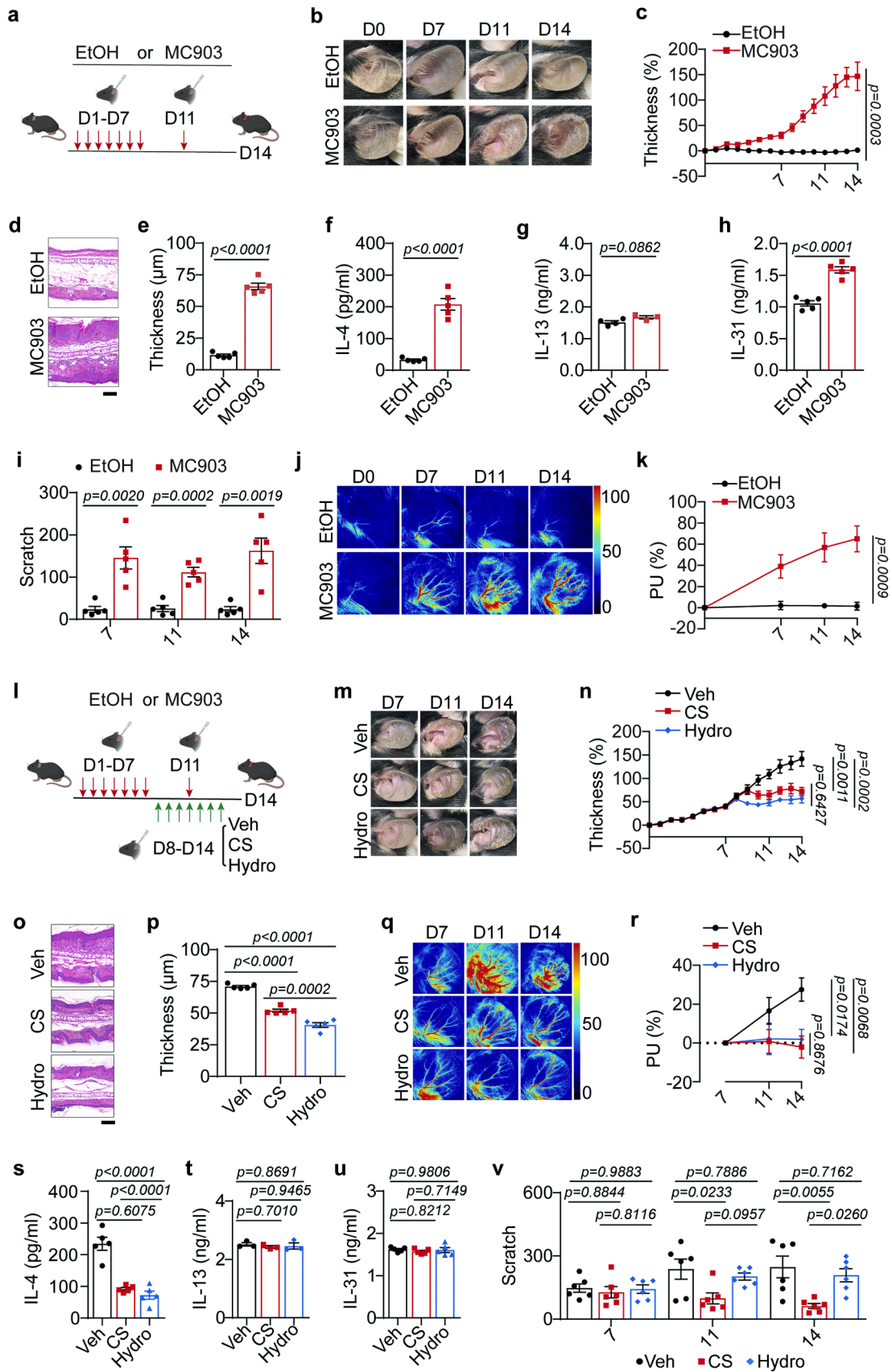
Quantification and statistical analysis

Data are presented as mean ± SEM. Data normality was determined by the Shapiro-Wilk test. Data that were normally distributed were then analyzed using a two-tailed *t*-test, while non-normality distributed data were analyzed with Mann-Whitney U test. Exact *P* value was indicated in the figures and *P* value less than 0.05 was considered statistically significant. As only male mice were studied, sex differences were not analyzed. Statistical analyses were conducted using Prism 10 software (GraphPad Prism 10, San Diego, CA, USA).

Results

A mouse model of AD flare-up exhibits skin inflammation, blood flow alteration, and itch

We employed a well-established murine model by topically administering calcipotriol (MC903) to mice on both ears for 7 days (Kim et al., 2019). Then, the treatment from day 8 to day 14 was ceased. On day 11, MC903 was administered once to simulate an AD flare-up (Fig. 1a). Compared to ethanol (EtOH), MC903 induced skin erythema (Fig. 1b) and edema, which was quantified by an increase in ear thickness



(caption on next page)

Fig. 1. CS ointment is sufficient to ameliorate skin inflammation and itch in AD-like mouse model. (a) Strategy for establishing AD-like mouse model. (b) Representative images illustrate distinct ear skin changes induced by MC903 treatment compared to vehicle control (EtOH). (c) Ear skin thickness variation is quantified in MC903- versus EtOH-treated mice. $n = 5$ mice per group. (d) Histological H&E staining reveals pathological alterations in ear skin after MC903 and EtOH administration on day 14 (scale bar = 100 μm). (e) Epidermal thickness measurements are presented for mice ears ($n = 5$ mice per group). (f-h) Lysate assays assess the expression of inflammatory cytokines IL-4 (f), IL-13 (g) and IL-31 (h) in ear skin on day 14 ($n = 3-5$ mice in each group). (i) Scratching behavior is quantified over a 30-minute interval for mice treated with EtOH or MC903 ($n = 5$ mice per group). (j-k) Laser speckle contrast imaging reveals elevated perfusion velocity in MC903-treated mice compared to EtOH controls (j), which is quantified in (k) (EtOH: $n = 5$ mice, MC903: $n = 4$ mice). (l) Treatment regimens involved daily application of vehicle, Chushizhiyang (CS) ointment, or hydrocortisone (Hydro) to AD-like mice from day 8 to day 14. (m) Representative images illustrate the appearance of mouse ears following treatment with vehicle, CS and hydrocortisone. (n) Ear thickness measurements were quantified in mice treated with vehicle ($n = 7$ mice), CS ($n = 8$ mice) and hydrocortisone ($n = 7$ mice). (o) Histological examination of ear skin sections obtained on day 14 after treatment with vehicle, CS and hydrocortisone revealed changes in tissue morphology (scale bar = 100 μm). (p) Epidermal thickness was measured in mouse ears ($n = 5$ mice per group). (q-r) Laser speckle contrast imaging detected decreased perfusion velocity in mice treated with CS and hydrocortisone, but not vehicle (q, quantified in r). Vehicle: $n = 5$ mice, CS, $n = 6$ mice, hydrocortisone: $n = 6$ mice. (s-u) Lysate assays analyzed the expression of inflammatory cytokines IL-4, IL-13, IL-31 in ear tissue samples collected on day 14 from mice treated with vehicle, CS and hydrocortisone on day 14 ($n = 3-5$ mice per group). (v) Scratching behavior was quantified over a 30-minute period in treated mice. $n = 6$ mice per group. All representative images represent multiple mice (minimum of three) per condition. Data are expressed as mean \pm SEM. Statistical significance is determined using two tailed Student's *t*-test (c, e, f, h, i, n, p, r, s, u, v) or Mann-Whitney U test (g, k, t).

(Fig. 1c) throughout the procedure. Histopathology validated these clinical findings as skin hematoxylin-eosin staining showed increased dermal thickening with infiltration of inflammatory cells (Fig. 1d and e). In the detection cytokines including IL-4, IL-13 and IL-31 in skin lysates, we found significantly elevated levels of IL-4 and IL-31 in MC903-treated animals compared to the EtOH controls (Fig. 1f-h), which mimic the clinical practice in AD patients (Bakker et al., 2023). Additionally, mice with AD-like disease experienced a significant increase in scratching bouts on the affected skin areas on day 7, 11, and 14 (Fig. 1i).

Previous studies suggest that morphology of blood vessels in erythematous skin of AD might be associated with skin inflammation (Tsutsumi et al., 2016). Using laser speckle contrast imaging that can reflect dermal perfusion (Linkous et al., 2023), we found a marked increase of skin blood flow in mice with AD-like disease (Fig. 1j and k). Taken together, these results indicate that mouse models with AD flare-up exhibited a significant presence of type 2 inflammation and increased blood flow in the skin.

CS ointment is sufficient to ameliorate skin inflammation and itch in AD

We next sought to investigate therapeutic effects of CS ointment on the AD model. Topical medications included CS ointment, vehicle ointment, and hydrocortisone ointment, which served as the positive control, were administered twice a day from day 8 to day 14 during the procedure (Fig. 1l). Strikingly, ear erythema and thickness were significantly reduced in mice administered with CS ointment than those treated with vehicle (Fig. 1m and n) in a dose-dependent manner (Supplementary Fig. 1a and b). These observations were confirmed by histopathology, which showed less inflammation infiltration and dermal thickness in the setting of CS ointment treatment (Fig. 1o and p, Supplementary Fig. 1c and d). Surprisingly, in addition to similar anti-inflammation effects (Fig. 1m-p), CS ointment exhibited comparable results in reducing skin hyper-perfusion with hydrocortisone (Fig. 1q and r, Supplementary Fig. 1e and f). Importantly, both CS ointment and hydrocortisone treatment decreased skin IL-4 levels (Fig. 1s, Supplementary Fig. 1h) with IL-13 and IL-31 unaltered (Fig. 1t and u, Supplementary Fig. 1i and j).

Regarding pruritus, we observed that mice treated with CS ointment showed a significant reduction of scratching bouts on day 11 and day 14 (Fig. 1v). The concentration of CS ointment and scratches exhibited a dose-dependent negative correlation (Supplementary Fig. 1g). The efficacy of CS treatment was significantly superior to that of steroid treatment, as seen by a marked reduction in scratching episodes on day 14 in mice treated with CS ointment compared to those treated with hydrocortisone. Collectively, the data suggests that CS ointment exhibited anti-inflammatory and anti-pruritic effects in the context of AD. However, the underlying mechanism remains unclear.

Network pharmacology predicts the potential targets of CS ointment on AD

CS ointment comprises 13 components (Supplementary Table 1) including *Cnidii Fructus*, *Coptidis Rhizoma*, *Phellodendri Chinensis Cortex*, *Dictamnii Cortex*, *Sophorae Flavescentis Radix*, *Polygoni Cuspidati Rhizoma et Radix*, *Violae Herba*, *Kochiae Fructus*, *Polygoni Avicularis Herba*, *Artemisiae Scopariae Herba*, *Atractylodis Rhizoma*, *Zanthoxylum bungeanum*, and *Borneol*. HPLC data indicated that the test sample we used in the study fit the reference standards according to the standard of China Food and Drug Administration (YBZ19482005) (Fig. 2a). Using TCM systems pharmacology (TCMSP), which is a database and analysis platform for TCM, 589 protein targets of CS ointment were predicted. An intersection with 1177 AD-related protein targets from Genecards, OMIM and DisGeNET database identified 173 shared protein targets (Fig. 2b). A protein-protein interaction (PPI) network was constructed based on the shared targets, consisting of 141 nodes and 1256 edges. Key proteins within the network include TNF, TP53, IL6, STAT3 and SRC (Fig. 2c). Furthermore, Gene Ontology (GO) enrichment analysis indicated that inflammatory response was a key biological process associated with CS ointment (Fig. 2d). Kyoto Encyclopedia of Genes and Genomes (KEGG) enrichment analysis suggested that inflammatory pathways, including the mediator regulation of TRP channels and cytokine-cytokine receptor interaction, play critical roles in alleviating AD mediated by CS ointment (Fig. 2e).

TRPM8-related pathways are associated with the effects of CS ointment

To depict a broad gene alteration that might be related to CS ointment-mediated effects, we performed bulk mRNA analysis in the ear skin in the setting of AD on day 14. Compared to vehicle control, while 205 upregulated and 294 downregulated genes were found in CS ointment-treated skin (Fig. 3a), hydrocortisone-treated skin showed 328 upregulated and 751 downregulated genes (Fig. 3b). However, comparison between the two groups revealed 271 upregulated and 159 downregulated genes (Fig. 3c), indicating their distinct mechanisms. In comparison to the untreated and vehicle ointments, CS ointment treatment down-regulated the expression of IL-4, IL-13, IL-31, IL-33, Ccl17 and Tslp in the skin by RT-PCR verification (Supplementary Fig. 2a-f). KEGG pathways enrichment analysis of differentially expressed genes (DEGs) identified several shared pathways (Fig. 3d and e) between the two medication groups. However, 125 altered genes (Fig. 3f) and 168 pathways (Fig. 3g) overlapped between CS ointment- and hydrocortisone-treated skin. Compared to the hydrocortisone-treated group, DEGs in the CS group were significantly enriched in pathways related to AD inflammation and pruritus, such as neuroactive ligand-receptor interaction, cytokine-cytokine receptor interaction, and chemokine signaling pathway (Fig. 3h). More importantly, further analysis of skin cytokines, chemokines, and pruritus-associated genes (Nattkemper et al., 2018) revealed the involvement of TRPM8-related

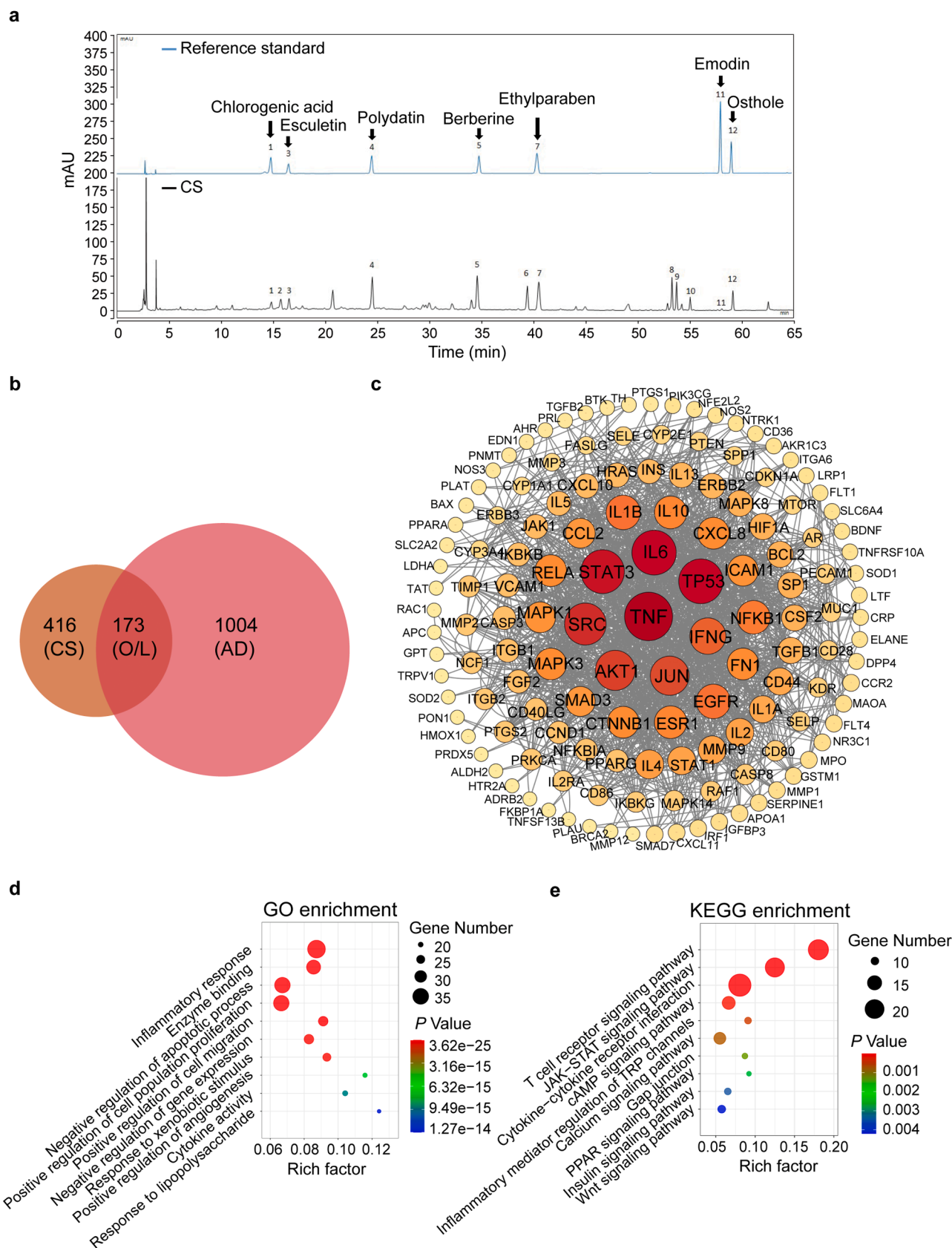


Fig. 2. Network pharmacology predicts the potential targets of CS ointment on AD. (a) The fingerprint of CS ointment. Mixture of seven reference substances: 1. Chlorogenic acid, 3. Esculetin, 4. Polydatin, 5. Berberine, 7. Ethylparaben, 11. Emodin, 12. Osthole. CS ointment is indicated by black line, reference standard by blue line. (b) A total of 589 protein targets of CS were predicted by using TCMSP database. One-hundred and seventy three shared protein targets were identified through intersections with AD-related protein targets collected in GeneCards, OMIM and DisGeNET database. (c) Protein-protein interaction network. (d) GO enrichment analysis. (e) KEGG enrichment analysis.

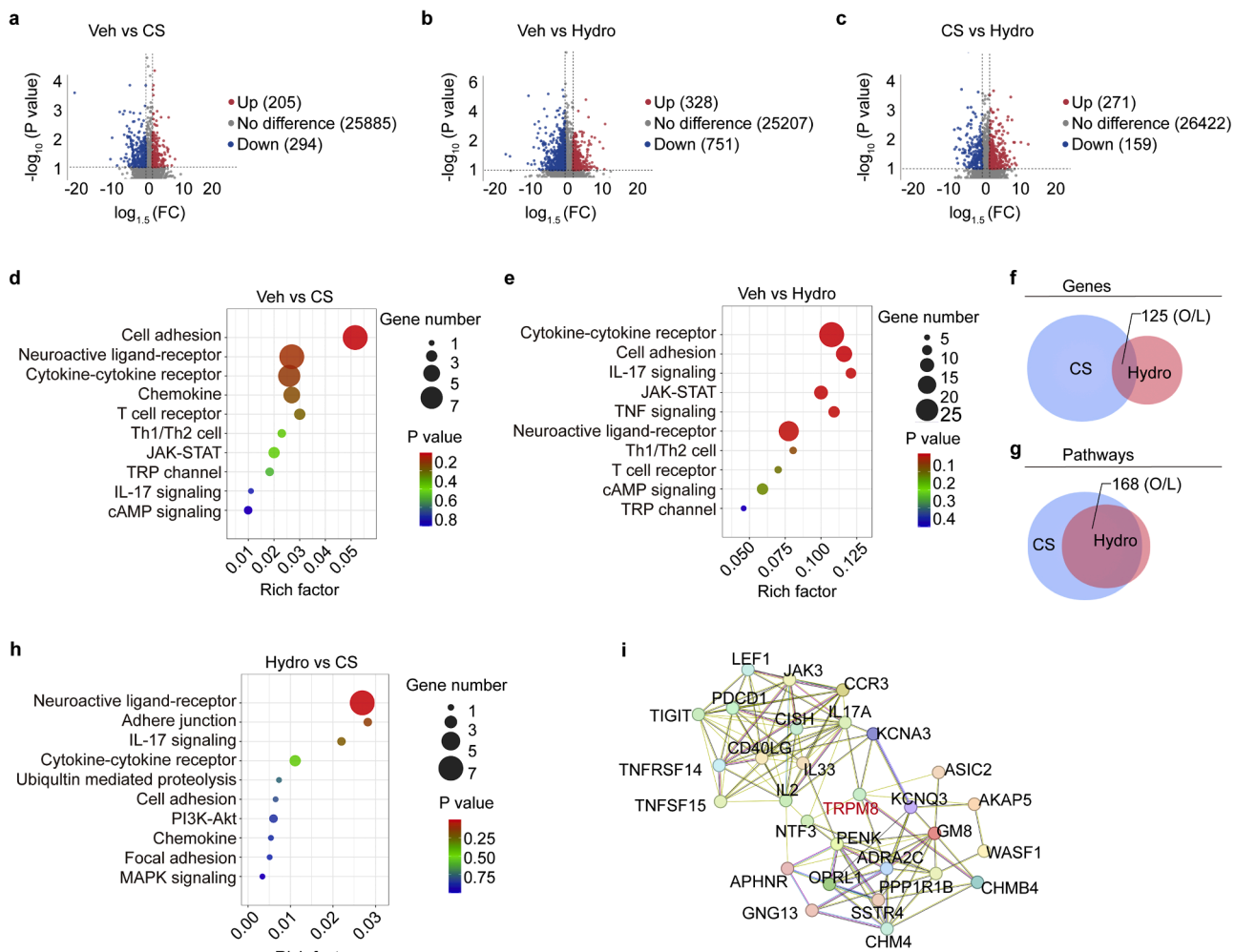


Fig. 3. TRPM8-related transcriptome changes were implied in CS ointment treatment. (a–c) Volcano plots depict differentially expressed genes (fold changes on X axis) through mRNA sequencing of ear tissues. Up-regulated genes are represented by red dots, while down-regulated genes are indicated by blue dots (a: vehicle versus CS, b: vehicle versus hydrocortisone, c: CS versus hydrocortisone). (d–e) KEGG enrichment analysis identified pathways related to inflammation and pruritus (d: vehicle versus CS, e: vehicle versus hydrocortisone). (f) The overlap of differentially expressed genes between vehicle and treatments including CS and hydrocortisone. (g) Differentially expressed genes between these samples revealed overlapping pathways. (h) KEGG enrichment analysis identified pathways related to inflammation and pruritus between CS and hydrocortisone treatments. (i) A protein–protein interaction network was visualized using STRING analysis.

pathways (Fig. 3i). Although the association is weak, considering that TRP plays an important role in disease development and process for cytokine releasing, we further focused on whether TRPM8 is involved in CS ointment-mediated effects.

CS ointment has the capacity to activate TRPM8-positive sensory neurons

Having found the distinctive changes in transcriptome profile that is related to neural pathways, we next sought to explore the role of neural TRPM8 in the effects of CS ointment. We employed a transgenic mouse line (Dhaka et al., 2007), in which enhanced green fluorescence protein (eGFP) was substituted for the functional TRPM8 protein under the *Trpm8* locus, thereby generating a knockout and reporter mouse line simultaneously (Fig. 4a). We used RT-PCR to verify *Trpm8* mRNA levels in the skin, which were significantly downregulated in *Trpm8*^{-/-} mice (Fig. 4b). After the visualization of TRPM8-positive fibers in the ear skin using whole-mount staining in *Trpm8*^{EGFP/+} transgenic mice (Fig. 4c), we injected fluoro-gold (FG, a neural tracer) into the mouse ear skin (Fig. 4d). After five days of injection, we observed a specific subset of neurons that express TRPM8 in the dorsal root ganglion (DRG) (Fig. 4e–h and k) and trigeminal ganglion (TG) (Fig. 4i–k).

We further performed calcium imaging with purified sensory

neurons in vitro as described previously (Li et al., 2019). As indicated, CS ointment diluted in calcium imaging buffer was sufficient to induce calcium influx in TRPM8-eGFP⁺ neurons that isolated from heterozygous *Trpm8*^{EGFP/+} mice in a dose-dependent manner (Supplementary Fig. 3a–e), whereas no alteration of calcium influx was revealed in those neurons from *Trpm8*^{-/-} animals (homozygous for *Trpm8*^{EGFP/+} genotype) (Fig. 4l–p). Collectively, these findings suggest that CS ointment specifically activates neuronal TRPM8. However, whether this characteristic contributes to its anti-inflammatory and anti-pruritic effects in AD remains unclear.

CS ointment-mediated effects are dependent on TRPM8 in AD

To test whether TRPM8 is required for the effects of CS ointment, we introduced *Trpm8*^{+/-} and *Trpm8*^{-/-} mice into our AD model, which showed similar levels of inflammation and itch (Supplementary Fig. 4). However, only *Trpm8*^{+/-} mice showed a therapeutic response to CS ointment. Ear thickness (Fig. 5a–d), skin blood flow (Fig. 5e and f), and scratching behavior (Fig. 5j) did not respond to CS ointment in *Trpm8*^{-/-} animals. Furthermore, skin IL-4 levels were significantly higher following CS ointment treatment in the TRPM8-deficient animals than those in *Trpm8*^{+/-} controls (Fig. 5g). Levels of skin IL-13 and IL-31

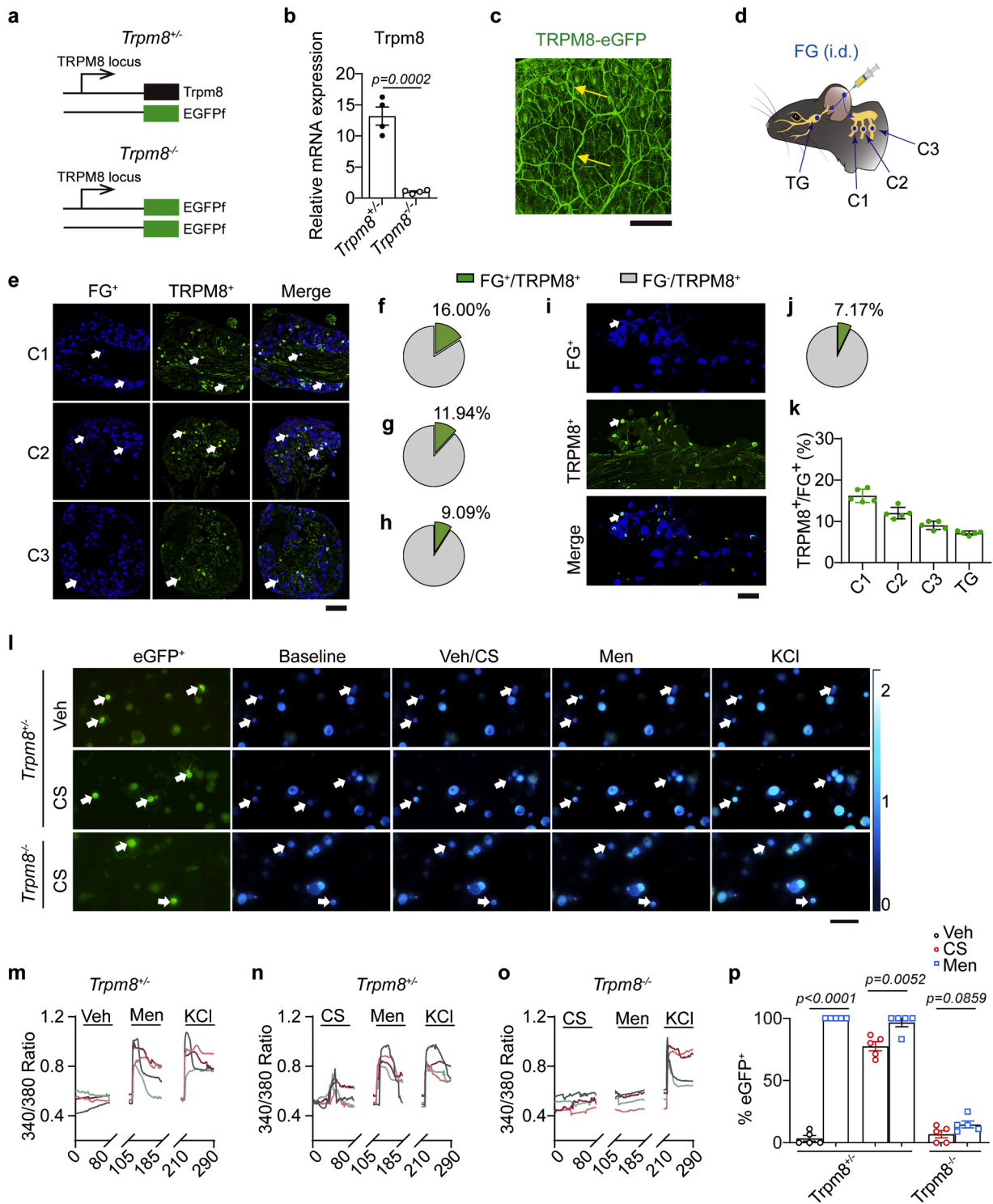


Fig. 4. CS ointment activates sensory TRPM8⁺ neurons. (a) Diagram indicates genetic strategy of *Trpm8*^{EGFPf/+} (*Trpm8*^{+/-}) transgenic mice, in which enhanced green fluorescence protein (eGFP) was substituted for the functional TRPM8 protein under the *Trpm8* locus, thereby generating a knockout (*Trpm8*^{-/-}) and reporter mouse line (TRPM8-eGFP) simultaneously. (b) RT-PCR validation of *Trpm8* in *Trpm8*^{+/-} and *Trpm8*^{-/-} mice. (c) Representative images of TRPM8-eGFP labeled sensory fibers, yellow arrows indicate TRPM8⁺ fibers in the ear skin of *Trpm8*^{EGFPf/+} mice. Scale bar = 500 μm. (d) Schematic diagram illustrates retrograde tracing by injecting a neural tracer, fluoro-gold (FG), into the mouse ear skin. (e) Representative images of TRPM8⁺ neurons labeled with FG in the dorsal root ganglion (C1-C3). Proportion is quantified in (f-h, k) (n = 5 mice, scale bar = 100 μm). (i) Representative images of TRPM8⁺ neurons labeled with FG in the trigeminal ganglion (Scale bar = 100 μm.). Quantification in (j, k) demonstrated overlapping (n = 5 mice per group). (l) TRPM8-eGFP labeled TRPM8⁺ sensory neurons cultured from *Trpm8*^{EGFPf/+} (*Trpm8*^{+/-}) mice exhibited responses to CS and menthol, but not to vehicle controls. No responses were observed in TRPM8-eGFP labeled neurons from *Trpm8*^{EGFPf/EGFPf} (*Trpm8*^{-/-}) mice. Neurons were sequentially stimulated with vehicle (0.1 mg/ml) or CS (0.1 mg/ml), menthol (100 μM) and KCl (50 μM). White arrows indicate TRPM8-eGFP neurons. Scale bar = 100 μm. (m-o) Representative calcium transients of sensory neurons from *Trpm8*^{+/-} and *Trpm8*^{-/-} mice in response to vehicle, CS, menthol (Men) and KCl are shown. Each colored trace represents one TRPM8-eGFP neuron. The images are representative of five independent experiments using dorsal root ganglion and trigeminal ganglion from at least three individual mice (m-o, quantified in p). Data are expressed as mean ± SEM. Statistical significance is determined using two tailed Student's *t*-test (b, p).

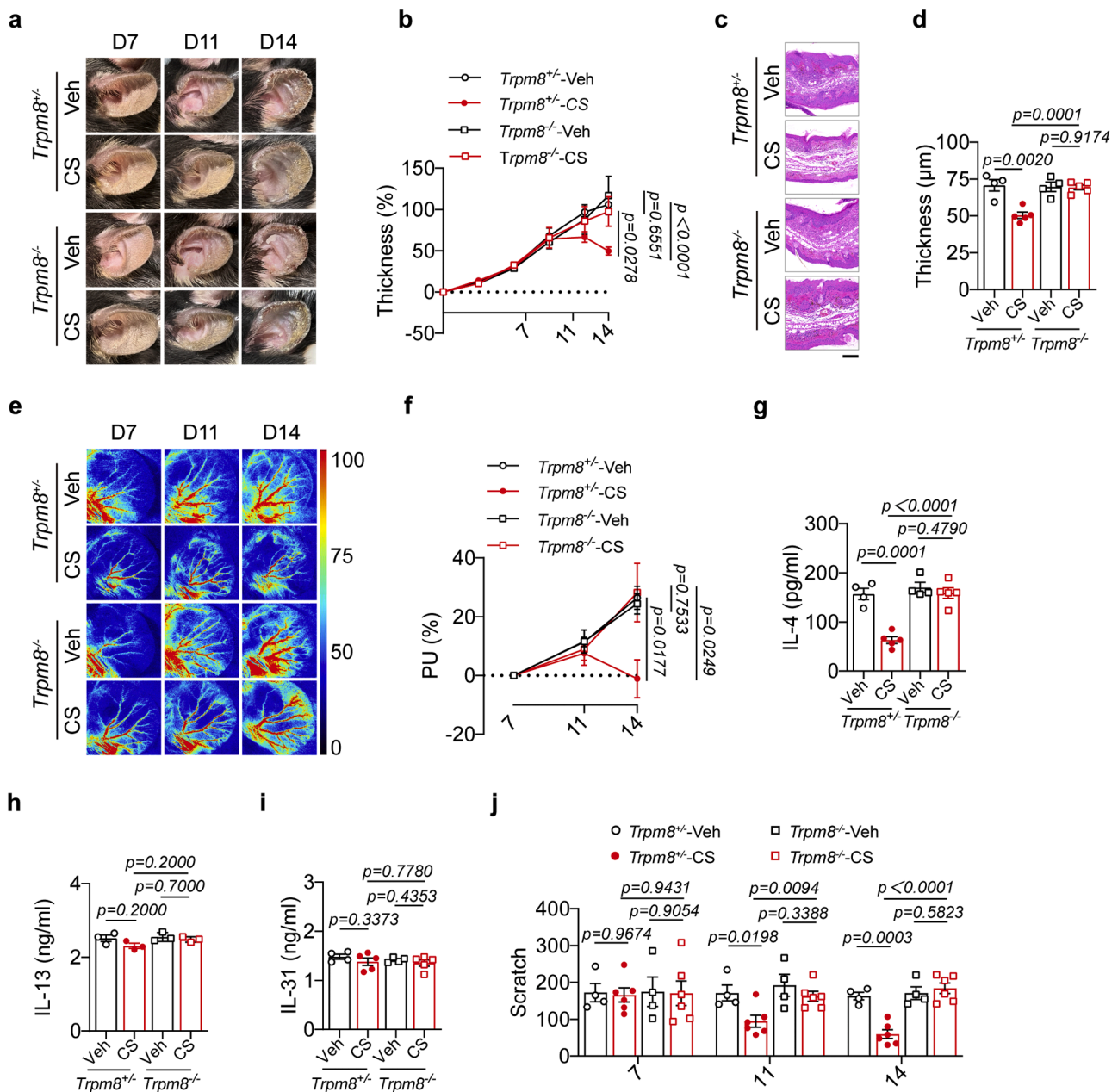


Fig. 5. TRPM8-deficiency abrogated the effects of CS ointment treatment in AD-like disease model. (a) Representative images show the ears of AD-like mice in *Trpm8*^{+/-} and *Trpm8*^{-/-} transgenic mice treated with vehicle and CS ointment. (b) Ear thickness changes were measured in AD-like mice in *Trpm8*^{+/-} and *Trpm8*^{-/-} mice receiving vehicle and CS treatment (n = 4–6 mice per group). (c–d) Histological changes in ear skin from *Trpm8*^{+/-} and *Trpm8*^{-/-} mice treated with vehicle and CS were examined on day 14. Scale bars = 100 µm. (c, quantified in d, n = 4–5 mice per group). (e–f) Laser speckle contrast imaging measurements revealed a significantly decreased perfusion velocity in *Trpm8*^{+/-}, but not *Trpm8*^{-/-} mice, after CS treatment (e, quantified in f; n = 4–5 mice per group). (g–i) Skin lysate assays of cytokines interleukin (IL)-4 (n = 4–5 per group), IL-13 (n = 3) and IL-31 (n = 4–5 per group) were performed on ear tissue from *Trpm8*^{+/-} and *Trpm8*^{-/-} mice after treatment. (j) Scratching behavior was observed over a 30-minute period in *Trpm8*^{+/-} and *Trpm8*^{-/-} mice treated with CS on day 7, day 11 and day 14 (n = 4–6 mice per group). All quantified data are expressed as mean ± SEM. Statistical significance is determined using two-tailed Student's *t*-test (b, d, f, g, h, j) or Mann-Whitney U test (h).

remained comparable between the two mice groups (Fig. 5h and i). Collectively, our findings indicate the essential role of TRPM8 in mediating the therapeutic effects of CS ointment in AD.

CS ointment suppresses sensory activities via TRPM8

It has been shown that hypersensitivities of sensory neurons are related to chronic pruritus (Liu et al., 2023; Meng et al., 2018). To investigate the neuronal status in our AD murine model, we examined the expression of pERK, a pan-marker of neural activities (Gao and Ji,

2009), in the DRG and TG. Notably, pERK was considerably upregulated in the small- and medium-diameter neurons in MC903-treated mice (Fig. 6a–d), indicating robust nociceptive activities in the context of AD. However, following the administration of CS ointment to the affected skin, there was a notable decrease in the percentage of pERK⁺ neurons (Fig. 6e–h). Remarkably, the deletion of *Trpm8* reversed the decrease effect of pERK expression, leading to a higher percentage of pERK⁺ neurons in *Trpm8*^{-/-} mice than those in *Trpm8*^{+/-} controls (Fig. 6i–l). Collectively, our findings reveal that CS ointment modulates the activities of sensory neurons through TRPM8, which is required for its

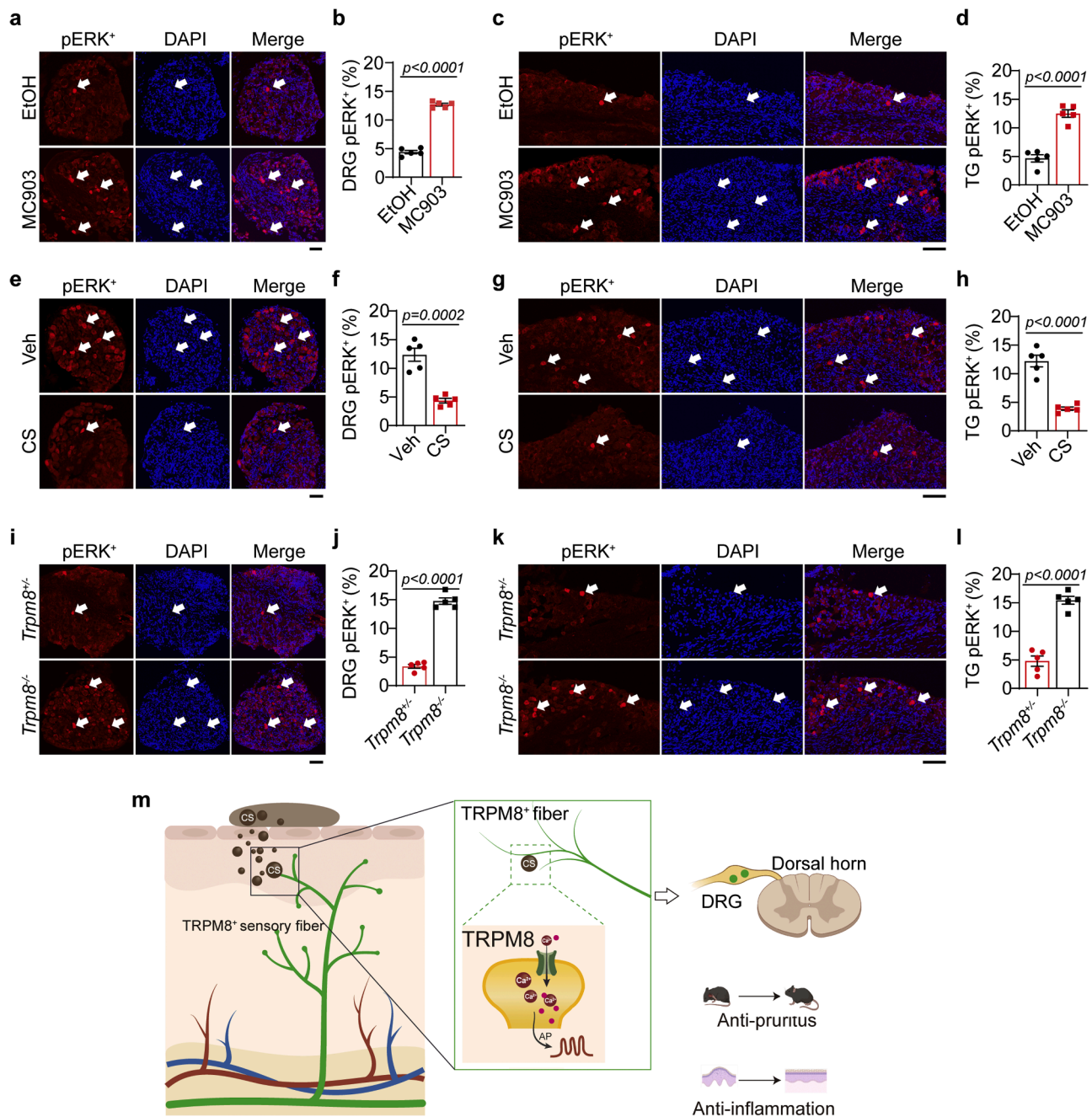


Fig. 6. TRPM8 is essential for the suppression of sensory activity by CS ointment. (**a-d**) Representative images of pERK immunofluorescence staining in cervical dorsal root ganglion (**a**, DRG; quantified in **b**) and trigeminal ganglion (**c**, TG; quantified in **d**) from MC903- and vehicle (EtOH)-treated mice. $n = 5$ mice per group. (**e-h**) Reduced pERK immunofluorescence signals were observed in CS ointment-treated DRG (**e**) and TG (**g**), but not in vehicle-treated controls (**e** quantified in **f**; **g** quantified in **h**; $n = 5$ mice per group). (**i-l**) Representative images of pERK immunofluorescence signals in *Trpm8*^{+/-} or *Trpm8*^{-/-} DRG (**i**) and TG (**k**) neurons after CS treatment. A decreased proportion of pERK⁺ neurons (**j**, DRG; **l**, TG) were observed in *Trpm8*^{+/-} but not *Trpm8*^{-/-} mice after CS treatment ($n = 5$ mice per group). (**m**) A schematic diagram illustrates the proposed mechanism by which the anti-inflammatory and anti-itch properties of CS ointment alleviate AD through TRPM8 activation. White arrows indicate pERK⁺ neurons in sensory ganglion. Scale bars = 100 μ m. Data presented as mean \pm SEM. Statistical analysis was performed using a two-tailed Student's *t*-test (**b**, **d**, **f**, **h**, **j**, **l**).

anti-inflammatory and anti-itch properties in treating AD-like disease (Fig. 6m).

Discussion

Our study demonstrates that CS ointment, a topical formulation composed of Chinese herbal ingredients, exhibits significant therapeutic effects in a murine model of AD. The application of CS ointment led to a marked reduction in skin thickness and scratching behavior, both of

which are hallmark features of AD. Furthermore, the ointment effectively lowered levels of type 2 cytokines, indicating a reduction in the inflammatory response, and improved blood flow in the affected areas. These findings suggest that CS ointment possesses both anti-pruritic and anti-inflammatory properties, which are crucial for managing AD. Notably, the superior itch-relieving effects of CS ointment compared to traditional topical steroid therapy highlight its potential as a safer alternative, particularly given the limitations and side effects associated with prolonged steroid use. A recent study (Zeng et al., 2024) has further

supported the efficacy of CS ointment in restoring skin microbiome homeostasis in AD mouse models. Collectively, this evidence positions CS ointment as a promising and effective therapeutic option for AD patients.

The therapeutic effects of CS ointment may be attributed to its composition, which includes 13 herbal components. Among these, berberine has been previously reported to alleviate eczema in mouse models when used in other formulations, such as Wenguanmu ointment (Zhu et al., 2023). Additionally, the TRP channel family, known to play a critical role in skin inflammation and pruritus (Mahmoud et al., 2022), appears to be a key target of CS ointment. For instance, borneol, a component derived from Chinese herbs, exerts anti-itch effects by activating the TRPM8 receptor, which induces a cooling sensation, while simultaneously inhibiting the TRPA1 pathway associated with inflammation and pain (Luo et al., 2024). Interestingly, our results indicate that TRPM8 itself may not be directly involved in the progression of AD, as both TRPM8 knockout (KO) mice and wild-type (WT) mice exhibited similar disease severity in terms of ear thickness and itch intensity. However, the anti-inflammatory and anti-pruritic effects of CS ointment were observed exclusively in WT mice with intact TRPM8 function, but not in TRPM8 KO mice. This suggests that while TRPM8 may not drive AD progression, its activation is essential for mediating the therapeutic effects of CS ointment, likely through its modulation of inflammation and itch pathways.

AD is characterized by a type 2-dominated immune response, leading to the overproduction of cytokines such as IL-4, IL-5, and IL-13 (Bakker et al., 2023). During the acute phase, excessive cytokine release triggers skin inflammation, impaired barrier function, vasodilation, and increased permeability. In the chronic phase, the infiltration of eosinophils and mast cells further exacerbates inflammation through the release of pro-inflammatory mediators like histamine and proteases, ultimately contributing to persistent skin thickening (Ständer, 2021). Therefore, controlling the acute phase of AD is critical to prevent disease progression. In this study, we employed calcipotriol (MC903) to establish and exacerbate an AD model, mimicking clinical disease manifestations. Treatment with CS ointment significantly reduced IL-4 cytokines levels during the acute phase, attenuated skin erythema, and improved skin blood flow. These results suggest that CS ointment is effective in managing early-stage AD symptoms, thereby reducing the risk of progression to the chronic phase and mitigating long-term complications associated with skin damage.

Our findings also underscore the critical role of TRPM8 ion channel in mediating the therapeutic effects of CS ointment. Although TRPM8-deficient mice exhibited similar initial AD-like symptoms as WT mice, the anti-inflammatory and anti-pruritic effects of CS ointment were absent in TRPM8 KO mice following treatment. This suggests that the therapeutic benefits of CS ointment are dependent on TRPM8 activation. The dual role of TRPM8 in inhibiting itch and reducing inflammation highlights its potential as a therapeutic target for AD (Fig. 6m). These findings align with the growing body of evidence emphasizing the importance of neuroimmune interactions in the pathogenesis of inflammatory skin diseases (Liu et al., 2023; Steinhoff et al., 2022). Thus, targeting TRPM8 may represent a promising strategy for AD treatment.

In conclusion, our study demonstrates that CS ointment represents a promising therapeutic approach for AD, exerting its beneficial effects through the modulation of TRPM8-mediated neuroimmune pathways. These findings not only provide new insights into the mechanisms underlying AD but also pave the way for the development of innovative treatments targeting the neuroimmune axis in chronic inflammatory skin conditions.

CRediT authorship contribution statement

Yao Chen: Writing – original draft, Project administration, Data curation. **Ziyuan Tang:** Project administration, Methodology, Data curation. **Zhiyao Han:** Formal analysis. **Mingyang Wang:** Formal

analysis. **Xinran Li:** Methodology. **Luying Lai:** Formal analysis. **Pingzheng Zhou:** Methodology. **Fang Wang:** Writing – review & editing, Conceptualization. **Fengxian Li:** Writing – review & editing, Writing – original draft, Supervision, Conceptualization.

Declaration of competing interest

The authors declare that they have no known competing financial interests or personal relationships that could have appeared to influence the work reported in this paper.

Acknowledgements

The authors acknowledge Dr. Zongxiang Tang of Nanjing Traditional Medicine University for providing *Trpm8*^{EGFPf} mice. This work was funded by Basic and Applied Basic Research Foundation of Guangdong Province (No. 2022A1515110168 to Luying Lai, No. 2024A1515010594 to Fengxian Li), and Yifan Pharmaceuticals (2023hxkt0501 to Fengxian Li). The investigated drug CS ointment was provided by Yifan Pharmaceuticals.

Supplementary materials

Supplementary material associated with this article can be found, in the online version, at doi:10.1016/j.phymed.2025.156524.

References

- Bakker, D., de Bruin-Weller, M., Drylewicz, J., van Wijk, F., Thijs, J., 2023. Biomarkers in atopic dermatitis. *J. Allergy Clin. Immunol.* 151 (5), 1163–1168. <https://doi.org/10.1016/j.jaci.2023.01.019>.
- Cai, X., Sun, X., Liu, L., Zhou, Y., Hong, S., Wang, J., Chen, J., Zhang, M., Wang, C., Lin, N., Li, S., Xu, R., Li, X., 2022. Efficacy and safety of Chinese herbal medicine for atopic dermatitis: evidence from eight high-quality randomized placebo-controlled trials. *Front. Pharmacol.* 13, 927304. <https://doi.org/10.3389/fphar.2022.927304>.
- Chu, C., Artis, D., Chiu, I.M., 2020. Neuro-immune interactions in the tissues. *Immunity* 52 (3), 464–474. <https://doi.org/10.1016/j.immuni.2020.02.017>.
- Dhaka, A., Murray, A.N., Mathur, J., Earley, T.J., Petrus, M.J., Patapoutian, A., 2007. TRPM8 is required for cold sensation in mice. *Neuron* 54 (3), 371–378. <https://doi.org/10.1016/j.neuron.2007.02.024>.
- Eichenfield, L.F., Tom, W.L., Berger, T.G., Krol, A., Paller, A.S., Schwarzenberger, K., Bergman, J.N., Chamlin, S.L., Cohen, D.E., Cooper, K.D., Cordoro, K.M., Davis, D.M., Feldman, S.R., Hanifin, J.M., Margolis, D.J., Silverman, R.A., Simpson, E.L., Williams, H.C., Elmets, C.A., Block, J., Harrod, C.G., Begolka, W.S., Sidbury, R., 2014. Guidelines of care for the management of atopic dermatitis: section 2. management and treatment of atopic dermatitis with topical therapies. *J. Am. Acad. Dermatol.* 71 (1), 116–132. <https://doi.org/10.1016/j.jaad.2014.03.023>.
- Gao, Y.J., Ji, R.R., 2009. c-fos and pERK, which is a better marker for neuronal activation and central sensitization after noxious stimulation and tissue injury? *Open. Pain. J.* 2, 11–17. <https://doi.org/10.2174/1876386300902010011>.
- Huang, X., Li, F., Wang, F., 2023. Neural regulation of innate immunity in inflammatory skin diseases. *Pharmaceuticals (Basel)* 16 (2). <https://doi.org/10.3390/ph16020246>.
- Kim, D., Kobayashi, T., Nagao, K., 2019. Research techniques made simple: mouse models of atopic dermatitis. *J. Invest. Dermatol.* 139 (5), 984–990. <https://doi.org/10.1016/j.jid.2019.02.014>. e981.
- Laughter, M.R., Maymone, M.B.C., Mashayekhi, S., Arents, B.W.M., Karimkhani, C., Langan, S.M., Dellavalle, R.P., Flohr, C., 2021. The global burden of atopic dermatitis: lessons from the global burden of disease study 1990–2017. *Br. J. Dermatol.* 184 (2), 304–309. <https://doi.org/10.1111/bjd.19580>.
- Li, F., Yang, W., Jiang, H., Guo, C., Huang, A.J.W., Hu, H., Liu, Q., 2019. TRPV1 activity and substance P release are required for corneal cold nociception. *Nat. Commun.* 10 (1), 5678. <https://doi.org/10.1038/s41467-019-13536-0>.
- Li, H., Zhang, Z., Zhang, H., Guo, Y., Yao, Z., 2021. Update on the pathogenesis and therapy of atopic dermatitis. *Clin. Rev. Allergy Immunol.* 61 (3), 324–338. <https://doi.org/10.1007/s12016-021-08880-3>.
- Linkous, C., Pagan, A.D., Shope, C., Andrews, L., Snyder, A., Ye, T., Valdebran, M., 2023. Applications of Laser Speckle contrast imaging technology in dermatology. *JID. Innov.* 3 (5), 100187. <https://doi.org/10.1016/j.xjidi.2023.100187>.
- Liu, A.W., Gillis, J.E., Sumpter, T.L., Kaplan, D.H., 2023. Neuroimmune interactions in atopic and allergic contact dermatitis. *J. Allergy Clin. Immunol.* 151 (5), 1169–1177. <https://doi.org/10.1016/j.jaci.2023.03.013>.
- Liu, B., Jordt, S.E., 2018. Cooling the itch via TRPM8. *J. Invest. Dermatol.* 138 (6), 1254–1256. <https://doi.org/10.1016/j.jid.2018.01.020>.
- Luger, T., Amagai, M., Dreno, B., Dagnelie, M.A., Liao, W., Kabashima, K., Schikowski, T., Proksch, E., Elias, P.M., Simon, M., Simpson, E., Grinich, E., Schmuth, M., 2021. Atopic dermatitis: role of the skin barrier, environment,

- microbiome, and therapeutic agents. *J. Dermatol. Sci.* 102 (3), 142–157. <https://doi.org/10.1016/j.jdermsci.2021.04.007>.
- Luo, M., He, J., Yin, L., Zhan, P., Zhao, Z., Xiong, H., Mei, Z., 2024. Borneol exerts its antipruritic effects by inhibiting TRPA1 and activating TRPM8. *J. Ethnopharmacol.* 322, 117581. <https://doi.org/10.1016/j.jep.2023.117581>.
- Mack, M.R., Kim, B.S., 2018. The itch-scratch cycle: a neuroimmune perspective. *Trends. Immunol.* 39 (12), 980–991. <https://doi.org/10.1016/j.it.2018.10.001>.
- Mahmoud, O., Soares, G.B., Yosipovitch, G., 2022. Transient receptor potential channels and itch. *Int. J. Mol. Sci.* 24 (1). <https://doi.org/10.3390/ijms24010420>.
- Meng, J., Moriyama, M., Feld, M., Buddenkotte, J., Buhl, T., Szöllösi, A., Zhang, J., Miller, P., Ghetti, A., Fischer, M., Reeh, P.W., Shan, C., Wang, J., Steinhoff, M., 2018. New mechanism underlying IL-31-induced atopic dermatitis. *J. Allergy Clin. Immunol.* 141 (5), 1677–1689. <https://doi.org/10.1016/j.jaci.2017.12.1002>.
- Misery, L., Santerre, A., Batardière, A., Hornez, N., Nedelec, A.S., Le Caër, F., Bourgeois, P., Huet, F., Neufang, G., 2019. Real-life study of anti-itching effects of a cream containing menthoxypropanediol, a TRPM8 agonist, in atopic dermatitis patients. *J. Eur. Acad. Dermatol. Venereol.* 33 (2), e67–e69. <https://doi.org/10.1111/jdv.15199>.
- Nattkemper, L.A., Tey, H.L., Valdes-Rodriguez, R., Lee, H., Mollanazar, N.K., Albornoz, C., Sanders, K.M., Yosipovitch, G., 2018. The genetics of chronic itch: gene expression in the skin of patients with atopic dermatitis and psoriasis with severe itch. *J. Invest. Dermatol.* 138 (6), 1311–1317. <https://doi.org/10.1016/j.jid.2017.12.029>.
- Peng, C., Yu, N., Ding, Y., Shi, Y., 2022. Epidemiological variations in global burden of atopic dermatitis: an analysis of trends from 1990 to 2019. *Allergy* 77 (9), 2843–2845. <https://doi.org/10.1111/all.15380>.
- Ständer, S., 2021. Atopic dermatitis. *N. Engl. J. Med.* 384 (12), 1136–1143. <https://doi.org/10.1056/NEJMra2023911>.
- Steinhoff, M., Ahmad, F., Pandey, A., Datsi, A., AlHammadi, A., Al-Khawaga, S., Al-Malki, A., Meng, J., Alam, M., Buddenkotte, J., 2022. Neuroimmune communication regulating pruritus in atopic dermatitis. *J. Allergy Clin. Immunol.* 149 (6), 1875–1898. <https://doi.org/10.1016/j.jaci.2022.03.010>.
- Tsutsumi, M., Fukuda, M., Kumamoto, J., Goto, M., Denda, S., Yamasaki, K., Aiba, S., Nagayama, M., Denda, M., 2016. Abnormal morphology of blood vessels in erythematous skin from atopic dermatitis patients. *Am. J. Dermatopathol.* 38 (5), 363–364. <https://doi.org/10.1097/dad.0000000000000373>.
- Wang, M.C., Chou, Y.T., Kao, M.C., Lin, Q.Y., Chang, S.Y., Chen, H.Y., 2023. Topical Chinese herbal medicine in treating atopic dermatitis (eczema): a systematic review and meta-analysis with core herbs exploration. *J. Ethnopharmacol.* 317, 116790. <https://doi.org/10.1016/j.jep.2023.116790>.
- Wang, W., Wang, H., Zhao, Z., Huang, X., Xiong, H., Mei, Z., 2020. Thymol activates TRPM8-mediated Ca²⁺ influx for its antipruritic effects and alleviates inflammatory response in Imiquimod-induced mice. *Toxicol. Appl. Pharmacol.* 407, 115247. <https://doi.org/10.1016/j.taap.2020.115247>.
- Wollenberg, A., Kinberger, M., Arents, B., Aszodi, N., Avila Valle, G., Barbarot, S., Bieber, T., Brough, H.A., Calzavara Pinton, P., Christen-Zäch, S., Deleuran, M., Dittmann, M., Dressler, C., Fink-Wagner, A.H., Fosse, N., Gáspár, K., Gerbens, L., Gieler, U., Girolomoni, G., Gregoriou, S., Mortz, C.G., Nast, A., Nygaard, U., Redding, M., Rehbinder, E.M., Ring, J., Rossi, M., Serra-Baldrich, E., Simon, D., Szalai, Z.Z., Szepietowski, J.C., Torreló, A., Werfel, T., Flohr, C., 2022. European guideline (EuroGuiDerm) on atopic eczema: part I - systemic therapy. *J. Eur. Acad. Dermatol. Venereol.* 36 (9), 1409–1431. <https://doi.org/10.1111/jdv.18345>.
- Zeng, B., Liu, X., Zhou, Y., Cui, G., An, L., Yang, Z., 2024. Effect of a topical traditional Chinese herbal medicine on skin microbiota in mouse model of atopic dermatitis. *Heliyon* 10 (13), e33240. <https://doi.org/10.1016/j.heliyon.2024.e33240>.
- Zhu, L., Li, X.J., Gu, C., Gao, Y., Zhang, C.S., Wang, L.Y., Chen, N.H., Li, G., 2023. Mongolian medicine Wenguanmu ointment treats eczema by inhibiting the CKLF-1/NF- κ B pathway. *J. Ethnopharmacol.* 313, 116549. <https://doi.org/10.1016/j.jep.2023.116549>.